ARMA 15-535

DEM simulation of fracture process of inherently anisotropic rock under Brazilian test condition

Kwok, C.Y. and Duan, K.
Department of Civil Engineering, The University of Hong Kong, Hong Kong

This paper was prepared for presentation at the 49th US Rock Mechanics / Geomechanics Symposium held in San Francisco, CA, USA, 28 June-1 July 2015.

ABSTRACT: Fracture process of inherently anisotropic rock discs under Brazilian test conditions are investigated with the use of two-dimensional Discrete Element Methods (DEM). In the DEM model, the rock matrix is represented as an assembly of rigid particles bonded at their contacts and the presence of intrinsic anisotropy is explicitly modeled by imposing individual smooth joint contacts into the bonded-particle model. A series of anisotropic models with different angles between weak layers and loading direction are tested (θ=0^o, 15^o, 30^o, 45^o, 60^o, 75^o, 90^o). The anisotropic numerical model is firstly calibrated to match the variation of Brazilian tensile strength with anisotropy angles of anisotropic rocks from published experimental data [1]. Good agreement can be found between the failure patterns of numerical model and those observed in laboratory. After that, the fracture process of anisotropic rock under diametrical compression is investigated in detail by exploring the occurrence, development and coalescence of micro cracks with different anisotropy angles. Micromechanical studies are also conducted by examining the modes, increment and distribution of micro cracks at different stages in order to gain insights on the failure mechanisms of anisotropic rocks under indirect tensile test conditions with different anisotropy angles.

1. INTRODUCTION

Among the many mechanical parameters, the tensile strength of rock material is a key one because rocks are in nature much weaker in tension than in compression. Many rock mechanics applications like the propagation of hydraulic fractures, rate of rock blasting, and drilling of boreholes in sedimentary rocks are highly dependent on the tensile strength of surrounding rocks [2, 3]. The Brazilian tensile test [4] (diametrical compression of circular discs) has been widely adopted in laboratory to determine the tensile strength of rock materials.

In laboratory, a series of experimental studies have been performed on different rocks with anisotropic properties in order to understand the responses of them under indirect tensile stress [5-8]. In fact, there is no consistent trend for the variation of Brazilian tensile strength (BTS) with the anisotropy angle due to the complex stress distribution between the weak layers and rock matrix. Based on results from nine types of rocks, Vervoort et al. [1] proposed four different trends for the BTS and failure patterns of anisotropic rocks under the Brazilain test conditions: trend1, the BTS stays constant over the entire anisotropy angles; trend 2, the BTS stays constant between 0^o and 45^o, followed by a linear decrease; trend 3, the BTS systematically decrease over the entire interval; trend 4: the BTS decreases from very low anisotropy angles (between 0^o and 30^o) and followed by a leveling off. They provided some explanations based on the relative lengths of fractures observed along the weak planes and in the matrix. However, the micromechanics for these different trends are still not fully understood. In addition, the failure patterns of anisotropic rocks are found more complex than those of isotropic rocks.

Several numerical approaches have been proposed to simulate the behaviors of anisotropic rocks under Brazilian test conditions [9-11]. However, each of them is adopted to represent just one specific rock type. No previous study can be found to look at the difference between different rocks. In this study, we attempt to explore how the weak layer properties affect the mechanical behaviors of anisotropic rocks exhibiting different trends with the use of Discrete Element Method (DEM).

This study presents a newly developed numerical approach [12] which can represent the weak layers normally encountered in anisotropic rocks at the micro-scale. The proposed numerical models are calibrated to represent four typical anisotropic rocks which belong to different trends. Based on the calibrated numerical models, differences between failure mechanisms are studied in detail. Particular attention is paid to the microscopic fracture process and mechanisms.

2. NUMERICAL METHODOLOGIES

The construction of a DEM model for anisotropic rock is depicted in Fig. 1. In the proposed model, the rock matrix is represented by bonding a series of rigid discs at their contacts (bonded-particle model). These discs can move independently with respect to each other. When the stress acting on the bond exceeds the related strength, the bond will break and the stress will be redistributed [13]. The smooth joint contact model is usually used to represent the fractures normally encountered in rock masses as particles can move along the smooth joint instead of slip around each other [14]. To represent the weak layers existing in anisotropic rocks, any parallel bonds dipping within a certain angle range will be replaced by a smooth joint model. This angle range can be tuned to represent rocks with different degree of anisotropy.

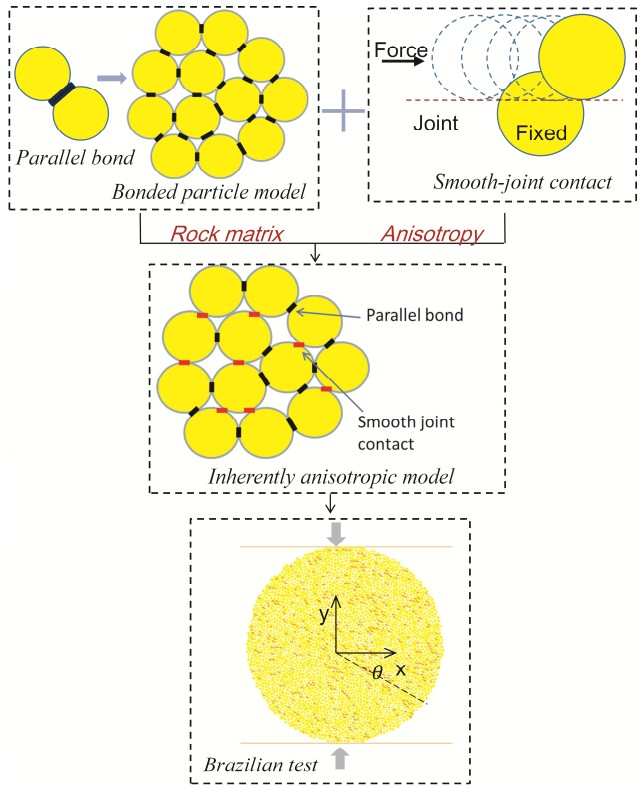

Fig.1. Construction of anisotropic rock model based on bonded particle model and smooth joint contact model. θ is the anisotropy angle.

Numerical samples with different anisotropy angles (θ=0°, 15°, 30°, 45°, 60°, 75°, and 90°) are constructed. Brazilian tests are conducted on these samples by moving the top and bottom platens with a constant velocity which is slow enough to ensure static. The force acting on the platens are measured and recorded. The tensile strength (σ_t) of the numerical model is calculated based on the following equation:

$$\sigma_t = \frac{P}{\pi R t} \tag{1}$$

where P is the maximum load, R is the radius of the Brazilan disc, and t is the thickness (1 for the 2D model). Since most anisotropic rocks fail in both tensile and shear modes [1, 6], σ_t does not always equals to the actual tensile strength, Eq. (1) will be mainly used for comparison purpose.

3. CALIBRATION

Similar with the bonded particle model for isotropic rocks, the micro parameters for this anisotropic rock model cannot be measured in the laboratory directly. Thus, a calibration procedure is necessary [15]. In this study, four typical rocks with different trends are selected to model, namely, the Postaer Sandstone (trend 1), the Boryeoung Shale (trend 2), the Leubsdorfer Gneiss (trend 3), and the Mosel Slate (trend 4). The calibrated micro parameters for these rocks are listed in Table 1. Fig. 2 compares the variation of BTS from simulated and experimental results versus anisotropy angles for the four different rocks. The Young's modulus obtained from uniaxial compression tests on cylinder sample when θ=0° and 90° are listed in Table 2.

As can be noted from Fig. 2 and Table 2, the proposed numerical approach can reproduce the mechanical responses of anisotropic rocks with different trends. Therefore, theses numerical models provide an avenue to investigate the difference lying in the micro-scale mechanisms of different anisotropic rocks.

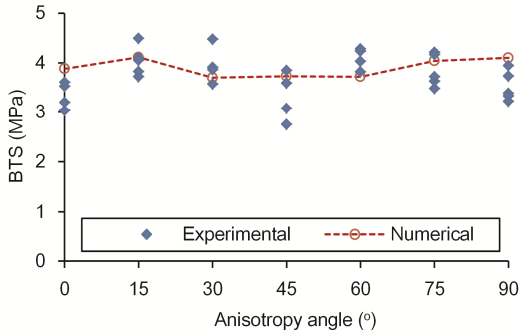

(a) Trend 1, Postaer Sandstone

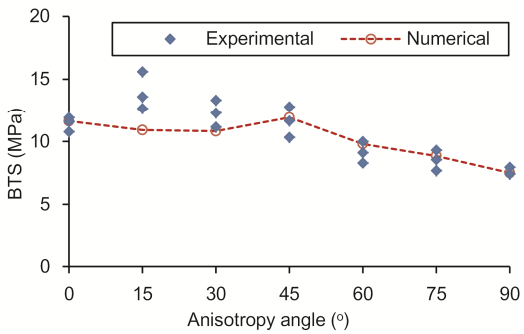

(b) Trend 2, Boryeoung Shale

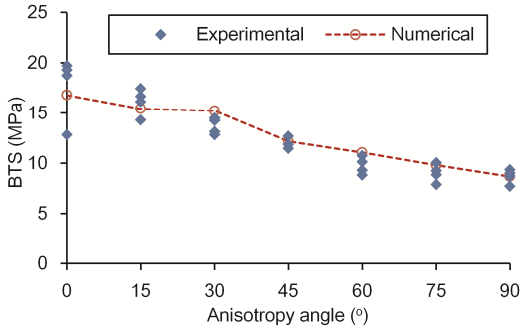

(c) Trend 3, Leubsdorfer Gneiss

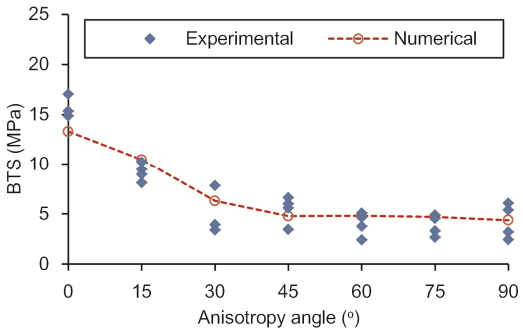

(d) Trend 4, Mosel Slate

Fig. 2. Variation of BTS versus anisotropy angles from simulated and experimental results for anisotropic rocks with different trends.

Table 1. Micro parameters calibrated for anisotropic rocks with different trends.

Microparameters		Postaer Sandstone	Boryeong Shale	Leubsdorfer Gneiss	Mosel Slate
Particle	$\bar{E}_c$(GPa)	22	33	66	110
Parallel bond	$\bar{E}_c$(GPa)	22	33	66	110
	$\bar{\sigma}_c$ (MPa)	17±4	62±14	85±20	100±23
	$\bar{\tau}_c$ (MPa)	17±4	62±14	85±20	100±23
Smooth-joint	Angle rang	±20°	±30°	±35°	±55°
	Normal stiffness, $\bar{k}_n$ (GPa/m)	55000	21000	80000	34000
	Shear stiffness, $\bar{k}_s$ (GPa/m)	55000	21000	80000	34000
	Tensile strength, σ_c (MPa)	17	5	10	7
	Cohesion, c_b	17	50	40	7
	Friction angle (φ)	0	0	30	0

Table 2. Young's modulus perpendicular and parallel to weak planes, determined on cylindrical specimens by uniaxial loading test

Rock	Experimental results [1]		Numerical results	
	E_0 (GPa)	E_90 (GPa)	E_0 (GPa)	E_90 (GPa)
Postaer Sandstone	-	27.9	27.8	28.5
Boryeong Shale	23.5	41.4	24.3	40.8
Leubsdorfer Gneiss	62.2	85.0	61.7	85.5
Mosel Slate	49.0	101.8	49.8	100.9

4. FAILURE PROCESS AND FAILURE MECHANICSMS

In the DEM model, micro-cracks can be divided into normal failure of parallel bond (crk_pb_n), shear failure of parallel bond (crk_pb_s), normal failure of smooth joint (crk_sj_n), and shear failure of smooth joint (crk_sj_s) according to their failure mechanism. Fig.3 presents the percentage of different cracks for the four anisotropic rocks with different anisotropy angles.

In these plots, cracks are divided into failure of parallel bond and failure of smooth joint. It can be noted from Fig. 3 that the dominant pattern of micro-cracks transforms from failure of parallel bond to failure of smooth joint from trend 1 to trend 4. Most micro cracks form as failure of parallel bond for Postaer Sandstone with all directions. Failure of smooth joint starts to take effect at high anisotropy angles for Boryeoung Shale. This trend becomes more significant for rock belongs to trend 3. As can be noted in Fig.3(c), 80% of cracks form as failure of smooth joint when θ exceeds 60°. Finally,

for Mosel Slate, failure of smooth joint takes place more than 80% for the entire interval.

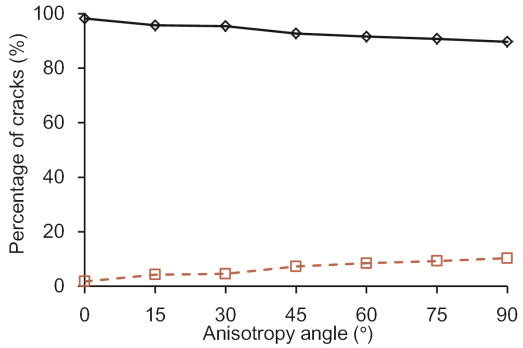

(a) Trend 1, Postaer Sandstone

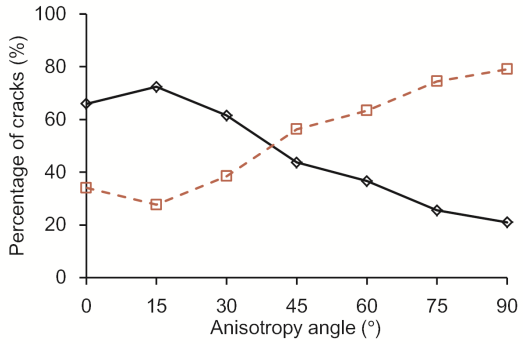

(b) Trend 2, Boryeoung Shale

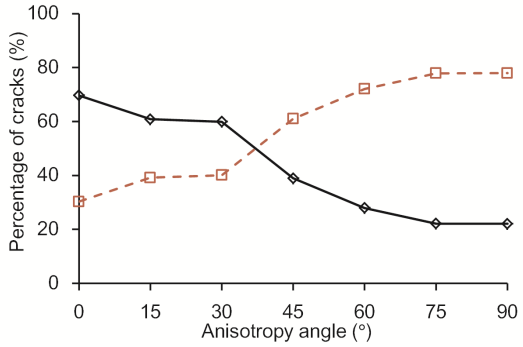

(c) Trend 3, Leubsdorfer Gneiss

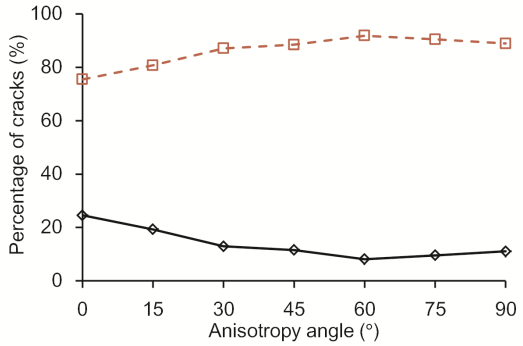

(d) Trend 4, Mosel Slate

Fig. 3 Percentage of micro-cracks for the four simulated rocks at 50% post-peak stage (solid line: failure of parallel bond; dash line: failure of smooth joint).

The percentage of different cracks agree well with the results from [1, 16] where fractures are classified as failure in the weak direction and other directions. The failure patterns and process of three simulated rocks with different degree of anisotropy (Postaer sandstone, Leubsdorfer Gneiss, and Mosel Slate) are investigated in detail.

4.1 Failure of Postaer Sandstone

The anisotropy ratio ($\sigma_{t,\max} / \sigma_{t,\min}$) of the Postaer Sandstone is 1.04, which is almost isotropic. As can be noted in Table 1, the strength of smooth joint is same with that of parallel bond. Therefore, the existence of weak layers does not affect the behaviors much, which is also confirmed by Fig. 3(a).

Distributions of micro-cracks for the simulated Postaer Sandstone at 50% post-peak stage are illustrated in Fig. 4. The fracture of simulated Postaer Sandstone with different anisotropy angles generally develop along the loading diameter. These fractures develop as results of failure of parallel bonds which have been demonstrated in Fig. 3(a). In other words, the effect of weak layers is not significant. These failure patterns provide evidence for the nearly constant variation of BTS. Similar failure modes have been observed on laminated sandstones [16].

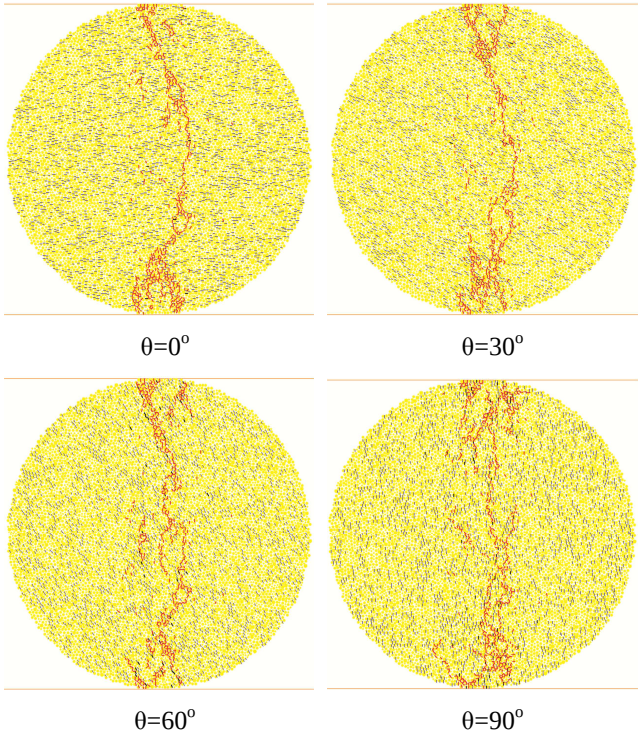

Fig.4 Failure patterns of simulated Postaer Sandstone. (Red lines: failure of parallel bond; Black line: failure of smooth joint)

4.2 Failure process of Leubsdorfer Gneiss

The anisotropy ratio of Leubsdorfer Gneiss equals to 0.49, which belongs to medium anisotropy [17]. The tensile stress versus vertical displacement curves for

simulated Leubsdorfer Gneiss with three different directions ($\theta=0^o$, 45^o, and 90^o) are plotted in Fig. 5, along with the increment of micro-cracks. The stress-displacement curves generally exhibit linear-elastic increase before peak, then, followed by a brittle drop at post-peak stage. The increment of micro-cracks varies with anisotropy angles. At low anisotropy angle ($\theta=0^o$), the effect of weak layers is minimum thus the failure mainly forms as tensile failure of parallel bonds. With the increase of anisotropy angle, more failure of smooth joint form before peak, but still considerable amount of tensile failure of parallel bond can be noted at post-peak stage (Fig. 5(b) and (c)).

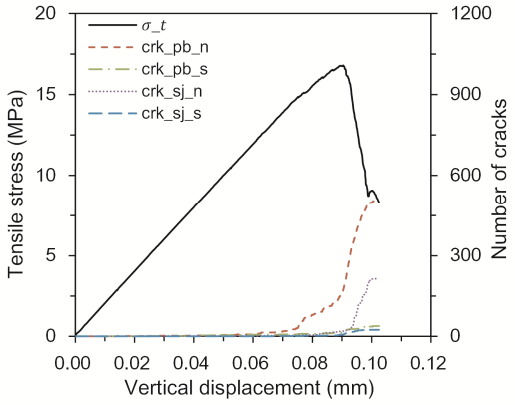

(a) $\theta=0^o$

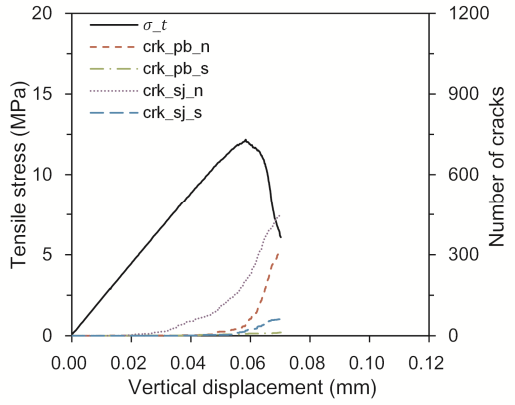

(b) $\theta=45^o$

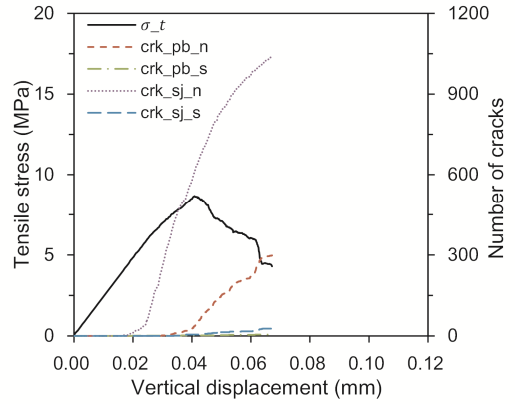

(c) $\theta=90^o$

Fig. 5 Stress-vertical displacement curves and increments of micro-cracks for simulated Leubsdorfer Gneiss.

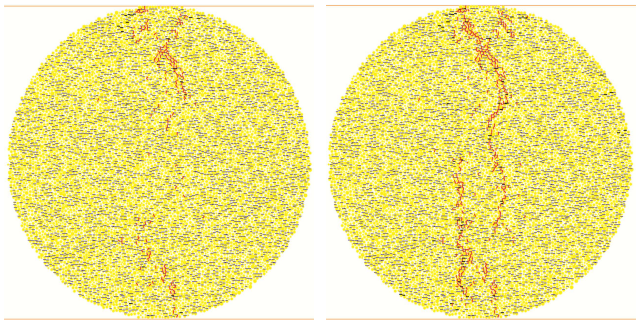

(a) $\theta=0^o$, peak $\theta=0^o$, post-peak

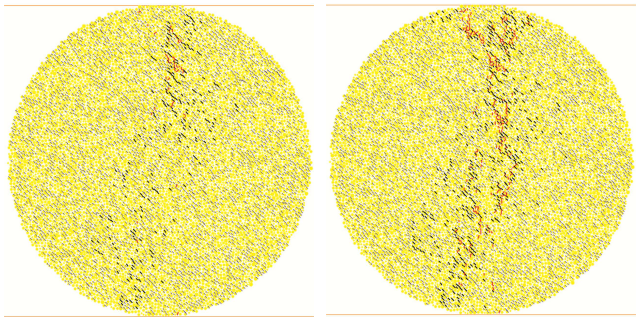

(b) $\theta=45^o$, peak $\theta=45^o$, post-peak

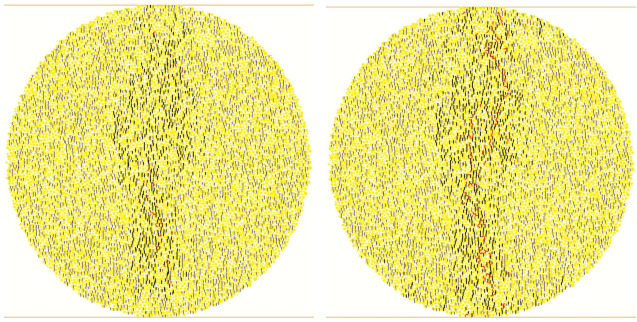

(c) $\theta=90^o$, peak $\theta=90^o$, post-peak

Fig. 6 Failure patterns of simulated Leubsdorfer Gneiss at different stages (red lines: failure of parallel bond; black lines: failure of smooth joint).

The fracture process of simulated Leubsdorfer Gneiss is illustrated in Fig. 6. When $\theta=0^o$, tensile failure of parallel bonds first appears at peak stage. Two meso-fractures can be observed near the top and bottom platens. The fractures develop vertically and finally a major fracture along loading diameter form at post-peak stage (Figure 6(a)). When $\theta=45^o$, tensile failure of smooth joint first occur, as can be noted in Fig 6(b). The existence of weak layers apparently disturbs the direction of fractures. A curved major fracture forms at post-peak stage as a result of failure of parallel bond, which connect the rock matrix. When $\theta=90^o$, a series of failures of smooth joints appear at peak stage around the center of disc but independently distributed. After peak stage, considerable number of tensile failures of parallel bonds occurs as can be noted in Fig.5 (c). It is the arising

of these failures in rock matrix splits the rock disc to two parts along the loading direction.

4.3 Failure process of Mosel Slate

The anisotropy ratio of Mosel Slate is 0.24, which belongs to heavy anisotropic rock. Different with the low and medium anisotropic rocks, the failure process of Mosel Slate presents a distinct mode.

Fig. 7 illustrates the tensile stress versus vertical displacement along with the increment of micro cracks for the simulated Mosel Slate when $\theta=0^o$. The stress-displacement curve is no longer linear elastic before peak but rather fluctuant. Notable failure of smooth joints and parallel bonds can be observed even at early stress stage (～70% of peak).

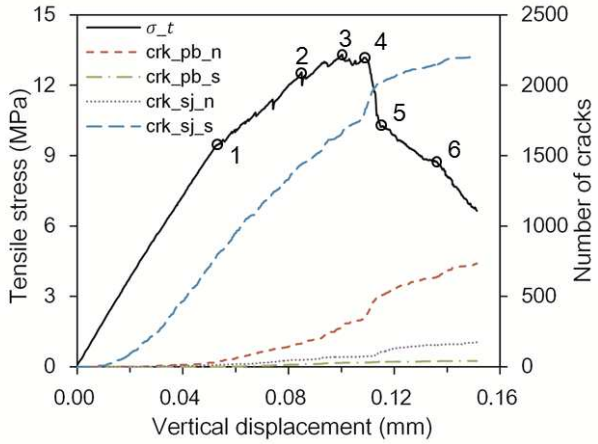

Fig. 7. Tensile stress versus vertical displacement and increment of micro cracks for simulated Mosel Slate. ($\theta=0^o$)

Fig. 8 illustrates the failure process of simulated Mosel Slate when $\theta=0^o$. Cracks first form near the top and bottom boundaries when the load reaches about 70% of peak in term of shear failure along weak layers. The behavior of the numerical model deviates from linear elastic as a result of these independent micro cracks. After this stage, tensile failure of parallel bond starts to form cross weak layers near top platen (red lines in Fig.8(b)). When the load reaches peak, significant increase of failure of smooth joints and parallel bonds can be noted in Fig 8(d). Macro-fracture near top platen can be noted. After this stage, the sample loses the capacity of carrying load and split along the loading direction (Fig.8(f)). Both the stress-displacement curve and the failure process described above agree well with the results from Vervoort et al. [8] on layered Slate.

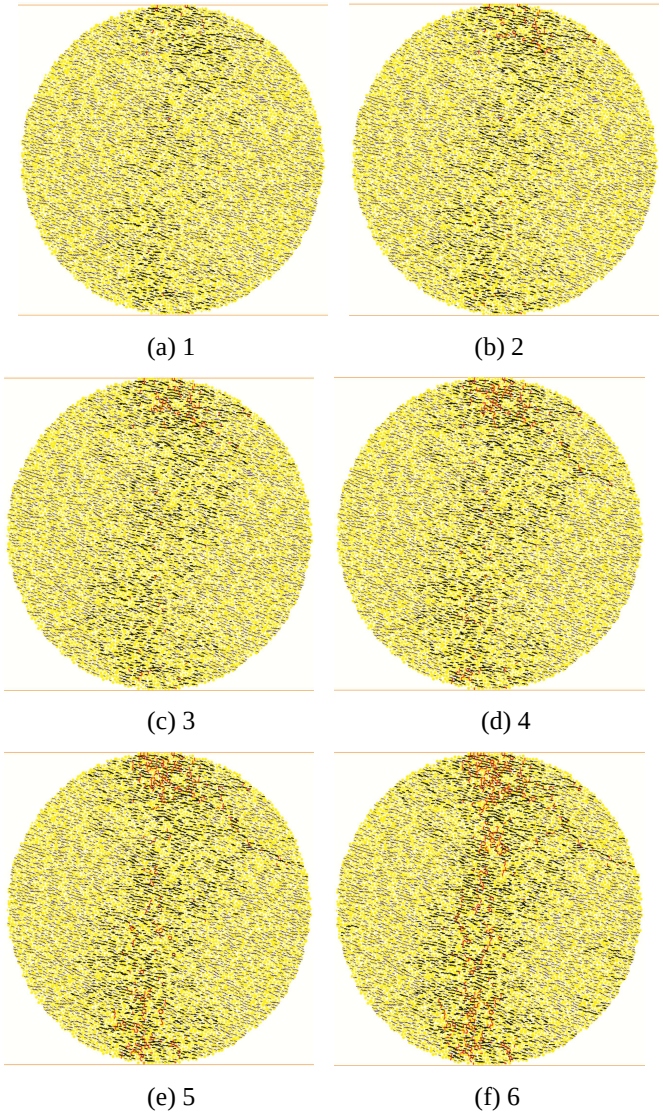

Fig. 8. Failure patterns of simulated Mosel Slate at different stages. The stages are marked in Fig. 7. ($\theta=0^o$, red lines: failure of parallel bond; black lines: failure of smooth joint)

5. CONCLUSIONS

The behaviors of anisotropic rocks under Brazilian test conditions are investigated in this study. In the numerical model, weak layers are explicitly represented by inserting smooth joint contacts into bonded particle model. The behaviors of anisotropic rocks with four trends are reproduced by this numerical model.

The failure process and failure mechanisms of three anisotropic rocks with different trends are examined and compared with experimental findings. It is the difference between the weak layers properties on particle scale controls the macroscopic failure strength and failure patterns. For low anisotropic rocks, the effect of weak layers is minor and failure occurs mainly along loading directions. For medium anisotropic rocks, the effect of weak layers becomes significant at intermediate loading directions. Fractures turn out to be curved as a result of

failure along weak layers. For heavy anisotropic rocks, the effect of weak layers becomes dominant even when loading applied perpendicular with weak layers. Fractures form as a results of shear failure along weak layers even at low anisotropy angles.

Innovative insights are provided based on the proposed numerical model in terms of the failure patterns of micro-cracks for rocks with different anisotropy ratios as a function of anisotropy angles. The micro parameters control the failure mechanisms on particle-scale, which ultimately determines the final failure strength and failure patterns with different anisotropy angles.

ACKNOWLEDGEMENT

The research was funded by the Natural Science Fund of China (NSFC) (Grant No. 51428902).

REFERENCES

1. Vervoort, A., et al. 2014. Failure of transversely isotropic rock under Brazilian test conditions. *International Journal of Rock Mechanics and Mining Sciences*, **70**: p. 343-352.
2. Zhang, J. 2013. Borehole stability analysis accounting for anisotropies in drilling to weak bedding planes. *International Journal of Rock Mechanics and Mining Sciences*, **60**(0): p. 160-170.
3. Amadei, B. 1996. Importance of anisotropy when estimating and measuring in situ stresses in rock. *International Journal of Rock Mechanics and Mining Sciences & Geomechanics Abstracts*, **33**(3): p. 293-325.
4. 1978. Suggested methods for determining tensile strength of rock materials. *International Journal of Rock Mechanics and Mining Sciences & Geomechanics Abstracts*, **15**(3): p. 99-103.
5. Chen, C.-S., E. Pan, and B. Amadei. 1998. Determination of deformability and tensile strength of anisotropic rock using Brazilian tests. *International Journal of Rock Mechanics and Mining Sciences*, **35**(1): p. 43-61.
6. Tavallali, A. and A. Vervoort. 2010. Failure of layered sandstone under Brazilian test conditions: effect of micro-scale parameters on macro-scale behaviour. *Rock mechanics and rock engineering*, **43**(5): p. 641-653.
7. Dan, D.Q., H. Konietzky, and M. Herbst. 2013. Brazilian tensile strength tests on some anisotropic rocks. *International Journal of Rock Mechanics and Mining Sciences*, **58**(Complete): p. 1-7.
8. Debecker, B. and A. Vervoort. 2009. Experimental observation of fracture patterns in layered slate. *International journal of fracture*, **159**(1): p. 51-62.
9. Tan, X., et al. 2014. Brazilian Tests on Transversely Isotropic Rocks: Laboratory Testing and Numerical Simulations. *Rock Mechanics and Rock Engineering*: p. 1-11.
10. Lisjak, A., et al. 2014. Numerical Modelling of the Anisotropic Mechanical Behaviour of Opalinus Clay at the Laboratory-Scale Using FEM/DEM. *Rock Mechanics and Rock Engineering*, **47**(1): p. 187-206.
11. Debecker, B. and A. Vervoort. 2013. Two-dimensional discrete element simulations of the fracture behaviour of slate. *International Journal of Rock Mechanics and Mining Sciences*, **61**: p. 161-170.
12. Kwok, C.Y., K. Duan, and L.G. Tham, 2014, Numerical simulation of strength and deformation behavior of inherently anisotropic rocks, in *48th US Rock Mechanics/Geomechanics SymposiumAmerican Rock Mechanics Association*: Minneapolis, MN, USA.
13. Potyondy, D.O. and P.A. Cundall. 2004. A bonded-particle model for rock. *International Journal of Rock Mechanics and Mining Sciences*, **41**(8): p. 1329-1364.
14. Ivars, D.M., et al. 2011. The synthetic rock mass approach for jointed rock mass modelling. *International Journal of Rock Mechanics and Mining Sciences*, **48**(2): p. 219-244.
15. Duan, K. and C. Kwok, 2015, Parametric study of smooth joint parameters on the behavior of inherently anisotropic rock under uniaxial compression condition, in *49th US Rock Mechanics/Geomechanics Symposium*: San Francisco.
16. Khanlari, G., B. Rafiei, and Y. Abdilor. 2014. An Experimental Investigation of the Brazilian Tensile Strength and Failure Patterns of Laminated Sandstones. *Rock Mechanics and Rock Engineering*: p. 1-10.
17. Ramamurthy, T., G.V. Rao, and J. Singh. 1993. Engineering behaviour of phyllites. *Engineering Geology*, **33**(3): p. 209-225.